



Artificial Intelligence-Enabled ECG to Detect Congenitally Corrected Transposition of the Great Arteries

Sunil J. Ghelani^{1,3} · Nikhil Thatte¹ · William La Cava² · John K. Triedman¹ · Joshua Mayourian¹

Received: 17 April 2025 / Accepted: 28 May 2025

© The Author(s), under exclusive licence to Springer Science+Business Media, LLC, part of Springer Nature 2025

Abstract

L-loop congenitally corrected transposition of the great arteries (ccTGA) is a rare congenital heart defect that may remain undiagnosed for decades and lead to significant morbidities, making it of interest for early detection. In this study, we address this gap by developing and internally testing an artificial intelligence-enabled electrocardiogram (AI-ECG) model to diagnose ccTGA from standard 12-lead ECGs. The dataset included the first ECG from 61,482 patients (0.7% with ccTGA), which was partitioned into training (70%) and testing (30%) cohorts. The convolutional neural network model achieved an area under the receiver-operating characteristic curve of 0.95 [95% CI 0.94–0.96] and an area under the precision-recall curve of 0.16 [95% CI 0.12–0.21]. The model performed well across different age groups, with slightly lower performance in patients < 1 month old. Key features identified by the model included widened QRS complexes, negative QRS complexes in leads V1-V2, and the lack of Q waves in lateral precordial leads. This study highlights the potential of AI-ECG to detect subtle patterns in rare congenital heart defects, providing a scalable method for early diagnosis and improving access to care. Future studies may include external validation in diverse clinical settings and multi-modal models to enhance performance and clinical utility.

Keywords Congenital heart disease · Artificial intelligence · Electrocardiograms · Congenitally corrected transposition of the great arteries

Introduction

L-loop congenitally corrected transposition of the great arteries (ccTGA) is a rare congenital heart defect characterized by atrioventricular and ventriculoarterial discordance that is conventionally detected by echocardiogram. Unlike the more common form of TGA (D-loop TGA) where immediate intervention is required, ccTGA can remain undiagnosed for many years in both resource-limited and resource-rich healthcare settings [1–5]. The progressive systemic right ventricular dysfunction, tricuspid regurgitation,

and arrhythmias that occur in ccTGA make timely diagnosis and management important [6]. Recent evidence demonstrated that early presentation of ccTGA for anatomic repair (i.e., double switch operation) is favorable for long-term outcomes. Therefore, timely diagnosis of ccTGA is of great interest [7].

Artificial intelligence-enabled ECG (AI-ECG) has shown promise as an inexpensive, ubiquitous, and noninvasive screening tool for detecting a range of pathologies in the general adult population, including structural heart diseases (e.g., hypertrophic cardiomyopathy and aortic stenosis) [8]. In the pediatric cardiology population, AI-ECG has also reliably detected numerous congenital heart lesions [9]. However, to our knowledge, an AI-ECG model has yet to be developed and validated to detect ccTGA.

In this study, we aimed to address this gap by developing and internally validating an AI-ECG model to detect ccTGA from standard 12-lead ECGs. To do so, we utilized a large, well-annotated, single-institution dataset and established deep learning techniques [10–12].

✉ Sunil J. Ghelani
sunil.ghelani@cardio.chboston.org

¹ Department of Cardiology, Harvard Medical School, Boston Children's Hospital, 300 Longwood Avenue, Boston, MA 02115, USA

² Department of Pediatrics, Computational Health Informatics Program, Harvard Medical School, Boston Children's Hospital, Boston, MA, USA

³ Department of Pediatrics, Harvard Medical School, Boston, MA, USA

Methods:

Study Population

Given our objective to detect ccTGA early in life, our inclusion criteria consisted of infants (≤ 1 years old) with ≥ 1 digitized ECG. We only included the first ECG per patient. ECGs failing to pass quality control were excluded. More specifically, ECGs were excluded if any lead contained fewer than 2500 samples or if any lead information was missing (1.0% exclusion rate). All ECGs were obtained from the cardiology database at Boston Children's Hospital, spanning from 1990 (earliest available digitized ECG) to 2023 [10, 11]. Patients were randomly assigned in a 70:30 ratio to training and internal testing sets, respectively.

Primary Outcomes

The primary outcome was confirmed diagnosis of L-loop ccTGA. This diagnosis is typically made by echocardiography; expert pediatric cardiology providers label patients with this diagnosis using a custom Fyler coding system [13]. This institutional coding system represents a well-established and standardized method for diagnostic classification. It is applied by experienced clinicians at our institution following comprehensive review of diagnostic data (including echocardiography). This diagnostic coding system has been successful for several AI-ECG applications, inclusive of detection of ventricular dysfunction and other forms of congenital heart disease [14, 15]. Rare forms of ccTGA (e.g., {I,D,D} situs inversus with atrioventricular and ventriculoarterial discordance) were not included in the case definition. Lesions commonly associated with ccTGA such as dextrocardia, Ebstein-like anomaly of the tricuspid valve, and ventricular septal defect were also identified using Fyler codes.

Data Retrieval and Processing

Raw ECG signals were extracted from the MUSE ECG management system (GE Healthcare, Chicago, IL), containing one-dimensional data vectors (sampling rate of 250 Hz for 10 s per lead). Leads III, aVF, aVL, and aVR were derived using Einthoven's law and the Goldberger equation [16, 17]. Additional retrieved data included age, sex, and the presence of dextrocardia, ventricular septal defect, or Ebstein-like malformation of the tricuspid valve.

High-pass filtering (cutoff frequency 0.8 Hz, rejection band 0.2 Hz, passband ripple 0.5 dB, rejection band attenuation 40 dB) was applied to remove artifacts such as baseline wander and electrical interference. ECGs were trimmed to 2048 samples (~8 s) to standardize input dimensions for a convolutional neural network.

Model Development, Training, and Evaluation

Two convolutional neural networks were trained to identify ccTGA. The first model received full 12-lead ECG inputs, aligning with standard clinical practice in the United States. In our literature review, we found that select international centers may use a subset of 9 leads (limb leads + V1, V3, V5) [9]. Therefore, to make our model compatible with select international practices, we also created a model that takes 9-lead inputs.

The training set was further divided, with 95% used for model training and 5% reserved for validation and hyperparameter tuning. The model architecture followed a residual network design adapted for one-dimensional signals [11]. Hyperparameter tuning was conducted using a grid search across kernel sizes [3, 9, 17], batch sizes [8, 32, 64], and initial learning rates [0.01, 0.001, 0.0001, 0.00001]. The final model was selected based on the lowest validation loss. The Adam optimizer was used to minimize cross-entropy loss over a maximum of 150 epochs, with early stopping based on validation performance. To reduce overfitting, a dropout rate of 0.2 was used.

Model performance was assessed using area under the receiver-operating characteristic (AUROC) and precision-recall (AUPRC) curves. Additional metrics such as positive predictive value (PPV), negative predictive value (NPV), sensitivity, and specificity were calculated using two clinically relevant cutoffs: 1) a high sensitivity cutoff (achieving 99% sensitivity); and 2) a high specificity cutoff (achieving 99% specificity). In addition, the model lift score was calculated, which is defined as the ratio of the PPV to the outcome prevalence. In other words, it measures how much better a model's predictions are compared to randomly guessing.

Bootstrap resampling (1000 iterations) was performed to obtain median values and 95% confidence intervals. Model performance was assessed in select age, sex, and lesion-specific subgroups. For subgroup analysis, the cohort was stratified into the following age groups: < 1 week, 1 week to 1 month, 1–3 months, 3–6 months, and 3 months to 1 year. Model performance was compared between the 12-lead ECG and 9-lead ECG using the DeLong test.

Model implementation used Keras with a TensorFlow backend in Python 3.9, with deep learning executed on institutional GPUs. Additional preprocessing and statistical analyses were conducted using Python 3.9 and R 4.0.

Model Explainability

To interpret model behavior, median waveform analysis and saliency mapping were employed as previously described [11]. Median waveforms provide visual representations of ECGs that are high- and low-risk of ccTGA. The 25 highest

predicted ECGs for ccTGA were used to generate high-risk median waveforms, and the 25 lowest predicted ECGs for ccTGA were used to generate low-risk median waveforms.

Saliency mapping highlights regions of the ECG that contribute to model predictions. Saliency maps were derived using Shapley Additive Explanations (SHAP) on the 25 ECGs with the highest predicted probability of ccTGA [18].

Results

Baseline Characteristics

The main study cohort included 61,482 patients, of whom 454 (0.7%) had ccTGA. Of those with ccTGA, 104 (23%) had dextrocardia, 49 (11%) had Ebstein-like malformation of the tricuspid valve, and 251 (55%) had a ventricular septal defect.

Table 1 Baseline characteristics of the training and testing datasets

	Training <i>N</i> = 43,074	Testing <i>N</i> = 18,408
Sex (male)	23,010 (53%)	9707 (53%)
Age at ECG (years)	0.2 (0.1, 0.4)	0.2 (0.1, 0.4)
Associated Lesions		
Dextrocardia	391 (0.9%)	182 (1.0%)
Ebstein	210 (0.5%)	81 (0.4%)
Ventricular septal defect	7105 (16%)	3033 (16%)
Outcome		
ccTGA	324 (0.8%)	130 (0.7%)

Baseline characteristics of the training ($n = 43,074$) and testing ($n = 18,408$) cohorts are shown in Table 1. Across both cohorts, 53% were male, and the median age at ECG was 0.2 [IQR 0.1–0.4] years. The prevalence of associated lesions such as dextrocardia, Ebstein-like anomaly of the tricuspid valve, and ventricular septal defect were 0.9–1%, 0.4–0.5%, and 16% across internal cohorts (Table 1).

Model Performance

As shown in Fig. 1, similarly high model performance is observed when using 12-lead (AUROC 0.95) and 9-lead inputs (AUROC 0.95) to detect ccTGA ($p = 0.41$). In the context of class imbalance and a ccTGA prevalence of 0.7%, an AUPRC of 0.16–0.17 was achieved.

Performance across subgroups, including age, sex, and associated lesions is presented in Fig. 2. AUROC and AUPRC remained consistent across ages 1 month to 1 year. Interestingly, performance slightly dropped in the 1 week to 1 month subgroup, and to a greater extent in the neonatal (< 1 week) subgroup. Model performance was slightly higher in males than females. In subgroups with dextrocardia, Ebstein-like malformation, and ventricular septal defect, the AUROC were lower and AUPRC higher.

Performance metrics were calculated when using high sensitivity and high specificity cutoffs (Table 2). At the high sensitivity cutoff (achieving 99% sensitivity), a specificity of 53%, NPV of 100%, PPV of 1.7%, and percentage predicted negative of 52.3% was obtained. At the high specificity cutoff (achieving 99% specificity), sensitivity was 36%, NPV was 99.5%, PPV was 20.3%, and percent predicted positive was 1.2%. At the high specificity cutoff, a lift score of 29 was achieved.

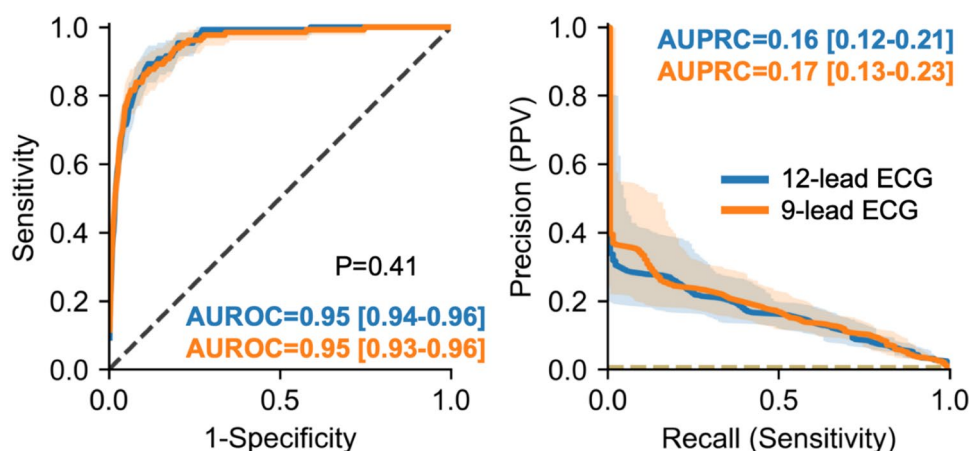


Fig. 1 AI-ECG Model Performance to Detect ccTGA. Receiver operative characteristics (left panel) and precision-recall (right panel) curves for the AI-ECG model for predicting the diagnosis of ccTGA using 12-lead ECGs (blue) versus 9-lead ECGs (orange). Dotted line represents chance. 95% confidence intervals are shown using boot-

strapping. P-value indicates comparison of 12-lead and 9-lead performance using the DeLong test. Abbreviations: AUROC, area under the receiver operative curve; AUPRC, area under the precision-recall curve; PPV, positive predictive value

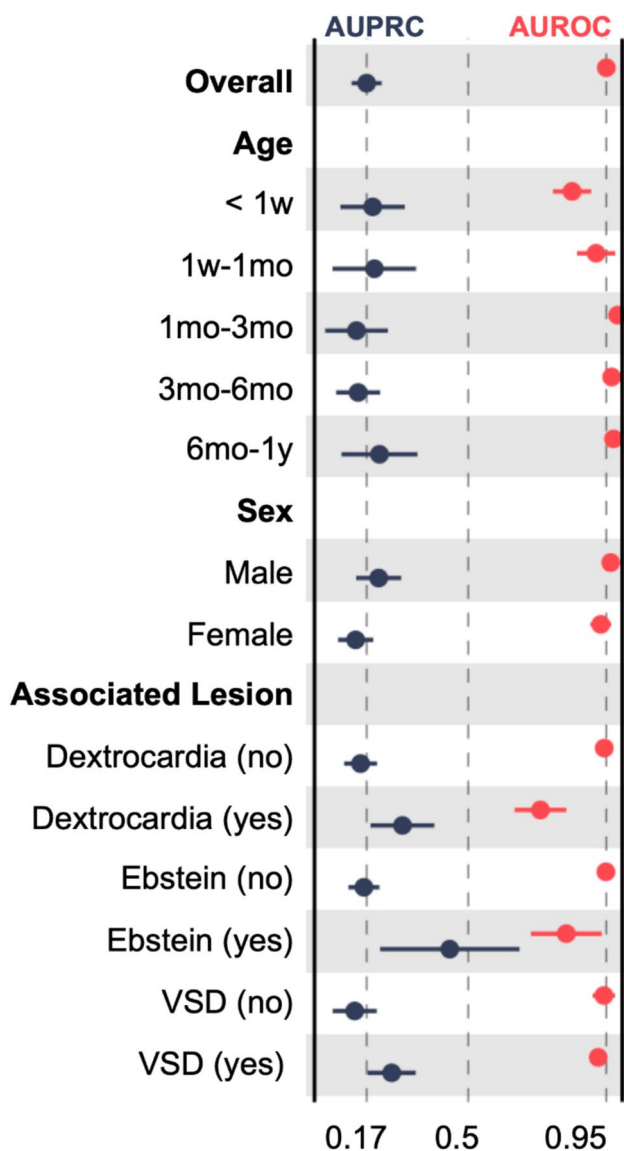


Fig. 2 Subgroup Analysis of AI-ECG Model Performance. Forest plot showing AI-ECG area under the receiver-operating (AUROC; red) and precision-recall (AUPRC; black) curve performance when stratifying by age group, sex, and associated lesions (dextrocardia, Ebstein-like malformation of the tricuspid valve, and ventricular septal defect)

Table 2 Performance metrics for AI-ECG model for detecting ccTGA

	High sensitivity cutoff	High specificity cutoff
Sensitivity	0.99 [0.97–0.99]	0.36 [0.27–0.45]
Specificity	0.53 [0.40–0.75]	0.99 [0.99–0.99]
NPV (%)	100.0 [100.0–100.0]	99.5 [99.5–99.6]
PPV (%)	1.7 [1.2–2.7]	20.3 [16.1–24.4]
Predicted Negative (%)	52.3 [39.9–74.0]	98.8 [98.7–98.8]

NPV negative predictive value; PPV positive predictive value

Model Explainability

To explain model behavior, median waveform analysis and saliency mapping was performed. Median waveforms for highest and lowest AI-ECG predictions are shown in Fig. 3. Waveforms that are high-risk for ccTGA include negative QRS complexes in V1-V2. In addition, wider QRS complexes are noted, with the absence of Q waves in lateral precordial leads. Salient features for predicting ccTGA include the QRS complex and T waves across limb (II, III, aVL, aVF) and precordial (V1-V2) leads.

Discussion

In this study, we developed and internally validated (to our knowledge) the first AI-ECG model to identify ccTGA from standard 12-lead ECGs. Our findings demonstrate the promise of AI-ECG for early detection of structural heart disease, and more broadly for children with congenital heart disease [9, 12, 19, 20]. Furthermore, our exploration of a model using a 9-lead subset (limb leads plus V1, V3, V5), informed by reported international ECG practices, demonstrated comparable diagnostic performance to the standard 12-lead approach. While requiring external validation, this suggests the potential feasibility of applying such AI-ECG tools in settings utilizing this reduced lead configuration, potentially broadening its applicability.

Clinical Relevance of Early ccTGA Detection

The optimal management of ccTGA remains unclear, especially among those with intact ventricular septum. One of the dilemmas for this lesion is the unpredictable nature of the systemic right ventricle. Recently, Cui et al. demonstrated that the natural history of ccTGA is challenging, with nearly half of ccTGA patients with intact ventricular septum developing varying degrees of right ventricular failure, tricuspid valve dysfunction, and premature death within 20 years of presentation [6, 21]. This same group demonstrated that early presentation of ccTGA for anatomic repair (i.e., double switch operation) is favorable (patients with presentation at age ≤ 5 years had a hazard ratio of 0.16 for a composite outcome of mortality, heart transplantation, or significant valvar or ventricular dysfunction after double switch operation) [6, 7].

AI-ECG Use for Detecting Structural Heart Disease

AI-ECG has been used to detect structural heart diseases in adults and to predict various forms of congenital heart disease in the pediatric population [9]. However, ccTGA is a rare condition, making the development of a tailored

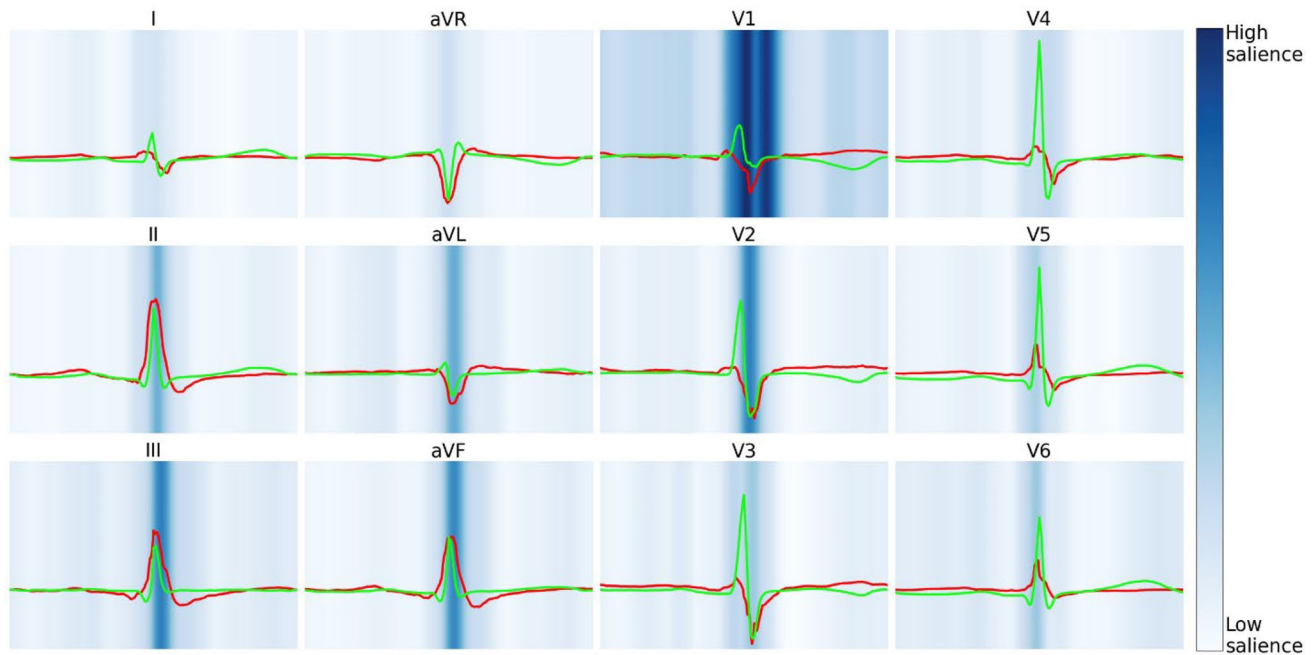


Fig. 3 AI-ECG Model Behavior to Predict ccTGA. Visualization of median waveforms generated in each lead using ECGs from the highest (red) and lowest (green) AI-ECG predictions of ccTGA. Saliency

mapping demarcates regions of the ECG waveform having greatest (dark blue) and least (light blue) influence to predict ccTGA

AI-ECG model difficult. In this study, we leveraged our institution's volume and data infrastructure to create a ccTGA-specific model. Our model explainability aligns with known ECG abnormalities in ccTGA (e.g., absence of Q waves in lateral precordial leads and abnormal depolarization of the interventricular septum) [22, 23]. These specific ECG characteristics are thought to reflect the underlying pathophysiology—the abnormal ventricular depolarization sequence resulting from ventricular inversion (atrioventricular discordance) and the altered spatial orientation of the heart.

Clinical Significance of this AI-ECG Tool

To assess the clinical relevance of our tool, we utilized two cutoffs: a high sensitivity cutoff, and a high specificity cutoff. While the high sensitivity cutoff achieves a high sensitivity (99%) and NPV (100%), only half of patients are predicted negative with a PPV of 1.7%. This low PPV indicates that the vast majority of positive results at this threshold would be false positives, potentially triggering a large volume of unnecessary follow-up echocardiograms. In a potential screening scenario, this would place a significant burden on healthcare resources, particularly impacting systems with limited echocardiographic capacity. In contrast, the high specificity cutoff achieves a specificity of 99% and PPV of 20%. In other words, in the select few that are deemed positive by AI-ECG (1.2%), 1 in 5 will then be confirmed to have

ccTGA. We feel this is a more clinically useful application of this technology, albeit it will only capture ~1/3 of cases (given the sensitivity of 36%).

Limitations and Future Directions

While these results are promising, we acknowledge several limitations. First, a primary limitation is that our model was developed and validated using data from a single-institution. Therefore, its generalizability to other clinical settings remains unproven, and external validation represents a crucial next step. Model performance may vary significantly when applied to external datasets due to potential differences in patient demographics, the prevalence of ccTGA and associated lesions, ECG acquisition systems (e.g., different manufacturers, software versions, filtering protocols), and data annotation practices. Future external validation studies are essential to assess the robustness and real-world applicability of this AI-ECG model. Second, our model requires access to digital waveforms. Recent work has demonstrated the potential of AI-ECG tools utilizing ECG photo inputs (rather than digital waveforms) [24]; future work may include creating a similar model to bypass the need for access to digital waveforms. Third, cost–benefit analyses and clinical implementation studies are required. Fourth, saliency mapping interpretations of model behavior are limited to the patients we studied and may change for unseen cases. Fifth, rare forms of ccTGA (e.g., {1,D,D} with

atrioventricular and ventriculoarterial discordance) were not included as positive cases. Finally, we acknowledge that model performance may improve if a multi-modal model was generated, inclusive of ECG, text, and/or imaging data.

Conclusion

In conclusion, this study demonstrates that AI-ECG can accurately detect ccTGA, offering a scalable way to improve early diagnosis and access to care. By identifying cases sooner, this tool may help ensure timely treatment and improve patient outcomes. Future research should focus on validating the model in different settings, integrating it into clinical practice, and exploring its potential for predicting long-term complications like RV failure and arrhythmias.

Acknowledgements The authors would like to acknowledge Boston Children's Hospital's High-Performance Computing Resources Clusters Enkefalos 3 (E3) made available for conducting the research reported in this publication.

Author Contributions S.G. and J.M. conceived and designed the study. J.M. curated the dataset, performed data preprocessing, and trained the AI model. All the authors contributed to data interpretation. S.G. and J.M. wrote the main manuscript text. All authors reviewed, edited, and approved the final manuscript.

Funding Kostin Innovation Fund (JM, JT, WGL), Thrasher Research Fund Early Career Award (JM), NHLBI T32HL007572 (JM), and Boston Children's Hospital Electrophysiology Research Education Fund (JM, JT.).

Data Availability No datasets were generated or analysed during the current study.

Declarations

Competing Interests The authors declare no competing interests.

References

- Sayuti KA, Azizi MY (2020) Incidental congenitally corrected transposition of the great arteries (ccTGA) in an adult with suspected coronary artery disease: review on radiological features and pathophysiology. *BMJ Case Rep* 13:e234225. <https://doi.org/10.1136/bcr-2019-234225>
- Osakada K, Ohya M, Waki K et al (2020) Congenitally corrected transposition of the great arteries at age 88 years. *CJC Open* 2:726–728. <https://doi.org/10.1016/j.cjco.2020.08.003>
- Wissocque L, Mondésert B, Dubart AE (2016) Late diagnosis of isolated congenitally corrected transposition of the great arteries in a 92-year old woman. *Eur J Cardiothorac Surg* 49:1524–1525. <https://doi.org/10.1093/ejcts/ezv379>
- Ono R, Takaoka H, Ryuzaki S et al (2022) Late presentation of congenitally corrected transposition of the great arteries. *BMJ Case Reports CP* 15:e248325. <https://doi.org/10.1136/bcr-2021-248325>
- Ferrero P, Chessa M, Varrica A, Giamberti A (2022) A case report of late physiologic repair of congenitally corrected transposition of the great arteries and pulmonary stenosis in a severely cyanotic patient: better late than never. *Eur Heart J* 6:ytab523. <https://doi.org/10.1093/ehjcr/ytab523>
- Cui H, Hage A, Piekarski BL et al (2021) Management of congenitally corrected transposition of the great arteries with intact ventricular septum: anatomic repair or palliative treatment? *Circ Cardiovasc Interv* 14:e010154. <https://doi.org/10.1161/CIRCINTERVENTIONS.120.010154>
- Marathe SP, Chávez M, Schulz A et al (2022) Contemporary outcomes of the double switch operation for congenitally corrected transposition of the great arteries. *J Thorac Cardiovasc Surg* 164:1980–1990.e7. <https://doi.org/10.1016/j.jtcvs.2022.01.049>
- Dhingra LS, Aminorroaya A, Sangha V et al (2025) Ensemble deep learning algorithm for structural heart disease screening using electrocardiographic images: PRESENT SHD. *J Am Coll Cardiol* 85:1302–1313. <https://doi.org/10.1016/j.jacc.2025.01.030>
- Chen J, Huang S, Zhang Y et al (2024) Congenital heart disease detection by pediatric electrocardiogram based deep learning integrated with human concepts. *Nat Commun* 15:976. <https://doi.org/10.1038/s41467-024-44930-y>
- Mayourian J, El-Bokl A, Lukyanenko P et al (2024) Electrocardiogram-based deep learning to predict mortality in paediatric and adult congenital heart disease. *Eur Heart J*. <https://doi.org/10.1093/eurheartj/ehae651>
- Mayourian J, Gearhart A, La Cava WG et al (2024) Deep learning-based electrocardiogram analysis predicts biventricular dysfunction and dilation in congenital heart disease. *J Am Coll Cardiol* 84:815–828. <https://doi.org/10.1016/j.jacc.2024.05.062>
- Mayourian J, La Cava WG, Vaid A et al (2024) Pediatric ECG-based deep learning to predict left ventricular dysfunction and remodeling. *Circulation*. <https://doi.org/10.1161/CIRCULATIONAHA.123.067750>
- Colan SD (2015) Early database initiatives: the flyer codes. In: Barach PR, Jacobs JP, Lipshultz SE, Laussen PC (eds) *Pediatric and congenital cardiac care, vol 1. Outcomes Analysis*. Springer, London, pp 163–169
- Mayourian J, La Cava WG, Vaid A et al (2024) Pediatric ECG-based deep learning to predict left ventricular dysfunction and remodeling. *Circulation* 149:917–931. <https://doi.org/10.1161/CIRCULATIONAHA.123.067750>
- Mayourian J, Geggel R, La Cava WG et al (2024) Pediatric electrocardiogram-based deep learning to predict secundum atrial septal defects. *Pediatr Cardiol*. <https://doi.org/10.1007/s00246-024-03540-7>
- Einthoven W, Fahr G, De Waart A (1950) On the direction and manifest size of the variations of potential in the human heart and on the influence of the position of the heart on the form of the electrocardiogram. *Am Heart J* 40:163–211. [https://doi.org/10.1016/0002-8703\(50\)90165-7](https://doi.org/10.1016/0002-8703(50)90165-7)
- Goldberger E (1942) A simple, indifferent, electrocardiographic electrode of zero potential and a technique of obtaining augmented, unipolar, extremity leads. *Am Heart J* 23:483–492. [https://doi.org/10.1016/S0002-8703\(42\)90293-X](https://doi.org/10.1016/S0002-8703(42)90293-X)
- Lundberg SM, Erion G, Chen H et al (2020) From local explanations to global understanding with explainable AI for trees. *Nat Mach Intell* 2:56–67. <https://doi.org/10.1038/s42256-019-0138-9>
- Hoodbhoy Z, Jiwani U, Sattar S et al (2021) Diagnostic accuracy of machine learning models to identify congenital heart disease: a meta-analysis. *Front Artif Intell* 4:708365. <https://doi.org/10.3389/frai.2021.708365>
- Anjewierden S, O'Sullivan D, Mangold KE et al (2024) Detection of right and left ventricular dysfunction in pediatric patients using artificial intelligence-enabled ECGs. *J Am Heart Assoc* 13:e035201. <https://doi.org/10.1161/JAHA.124.035201>

21. Barron DJ, Guariento A (2021) Strengthening the argument for the double switch: but where is the limit? *Circ Cardiovasc Interv* 14:e010888. <https://doi.org/10.1161/CIRCINTERVENTIONS.121.010888>
22. Fernández F, Laurichesse J, Scebat L, Lenègre J (1970) Electrocardiogram in corrected transposition of the great vessels of the bulbo-ventricular inversion type. *Br Heart J* 32:165–171. <https://doi.org/10.1136/hrt.32.2.165>
23. Almasri M, Salim H, Orcutt J (2023) What is the diagnosis? *Eur Heart J* 7:ytad446. <https://doi.org/10.1093/ehjcr/ytad446>
24. Sangha V, Mortazavi BJ, Haimovich AD et al (2022) Automated multilabel diagnosis on electrocardiographic images

and signals. *Nat Commun* 13:1583. <https://doi.org/10.1038/s41467-022-29153-3>

Publisher's Note Springer Nature remains neutral with regard to jurisdictional claims in published maps and institutional affiliations.

Springer Nature or its licensor (e.g. a society or other partner) holds exclusive rights to this article under a publishing agreement with the author(s) or other rightsholder(s); author self-archiving of the accepted manuscript version of this article is solely governed by the terms of such publishing agreement and applicable law.